

Received February 26, 2021, accepted March 9, 2021, date of publication March 25, 2021, date of current version May 24, 2021.

Digital Object Identifier 10.1109/ACCESS.2021.3068054

# Comprehensive Analysis of Winding Electromagnetic Force and Deformation During No-Load Closing and Short-Circuiting of Power Transformers

CHENCHEN ZHANG<sup>1</sup>, WENQI GE<sup>1</sup>, YI XIE<sup>1</sup>, AND YINGYING LI<sup>1,2</sup>

<sup>1</sup>School of Control and Mechanical Engineering, Tianjin Chengjian University, Tianjin 300384, China

<sup>2</sup>Tianjin Research Institute of Construction Machinery, Tianjin 300409, China

Corresponding author: Wenqi Ge (gewenqi@tcu.edu.cn)

This work was supported by the National Science Foundation for Young Scientists of China under Grant 51707128.


**ABSTRACT** When an electromagnetic transient occurs in a transformer, certain parts of the winding will be over stressed internally, which in severe cases will lead to the destruction of the winding insulation. Excitation inrush current and short-circuit current are the main causes of winding damage during electromagnetic transients, resulting in or accelerating winding damage, and the presence of short-circuit current and excitation inrush current can greatly reduce the service life of power transformers. The process of closing and energizing a transformer generates a large excitation inrush, and when the current amplitude is the same, the excitation inrush generates a greater electromagnetic force than the short-circuit current. In this paper, the field-path coupling method and the finite element method (FEM) are combined to analyze the magnetomechanical effects on the transformer winding through the principle analysis and simulation, comparing the excitation inrush and short-circuit current scenarios, analyzing and concluding the leakage characteristics of the excitation inrush and short-circuit current and the winding force deformation results.

**INDEX TERMS** Excitation inrush, short-circuit current, electromagnetic force, magnetomechanical effect.

## I. INTRODUCTION

Transformers are an important component of the power system for the transmission of electricity and are more expensive to maintain and monitor than other power generation and transmission equipment. When a transformer is damaged, it not only incurs high repair or replacement costs but may also result in greater economic losses due to the temporary loss of power transmission capacity of the power system. Therefore, for the safe and stable operation of the power system, power transformers need to be studied for failure prevention to avoid affecting normal power transmission.

The power transformer faults studied in this paper refer mainly to the winding vibrations caused by electromagnetic forces in the presence of high currents and the resulting damage to the insulation between the transformer windings. One of the first concerns and discussions about this phenomenon was the high current action of short-circuit currents.

The associate editor coordinating the review of this manuscript and approving it for publication was Hui Ma .

The literature [1] used the field-path coupling method to calculate the leakage magnetic field and the short-circuit electromagnetic force under short-circuit conditions, and the winding flexure analysis according to the actual parameters to study the spoke stability of the winding. Transient analysis is used to determine the location of maximum transformer winding deformation, and dynamics analysis is performed at this location to determine whether spoke instability will occur. In [2], a comparative analysis of the low-voltage winding of a dual-winding transformer with a distributed structure under different short-circuit conditions was carried out using the field-path coupling method, and the leakage and the electromagnetic forces generated in each case were analyzed. The literature [3], [4] analyses the electromagnetic characteristics of the transformer windings and the dynamic characteristics of the electromagnetic forces in the case of short-circuit current shocks using the finite element method. The variation patterns of the winding forces and displacements were obtained, and the electromagnetic forces and displacements on the middle and both ends of the winding were compared.

In the literature [5], the effect of the width of the spacer on the critical yield stress of the winding was analyzed using the finite element method, and a method for calculating the critical yield stress of the transformer winding was proposed.

In some cases, the no-load operation of the transformer will produce a large excitation inrush current, the duration of the excitation inrush current can reach tens of seconds, its amplitude not only far exceeds the rated current of the transformer, and even exceed the peak short-circuit current. Excessive excitation inrush current can lead to transformer winding deformation, damage winding insulation, and cause differential protection false operation, affecting the safe and stable operation of the power system. Normally, transformers are tested for short-circuit resistance, but tests relating to transformer excitation inrush currents are not abundant.

At present, research on transformer excitation inrush is focused on the identification of the excitation current flow, and a series of research results have been achieved. In [6] a new controlled switching control strategy is proposed to reduce the excitation inrush taking into account core saturation and residual flux. A transient transformer model based on electrical and magnetic circuits is also proposed. A comparison of experimental and simulation results shows that the above proposed scheme can effectively reduce the excitation inrush current. However, the non-linearity, randomness, and diversity of the excitation current make the existing solutions imperfect.

It is important to study in-depth the mechanism of the generation of excitation inrush current and to fully grasp the law of its variation, the effect on the transformer winding, and the difference with the short-circuit current. In the literature [7] a mathematical expression for the transient variation of the magnetic field is obtained by solving a differential equation. At the same time, the expression is expressed as an alternative form of the iterative equation. Through simulation, the flux and current relationship curves are obtained and the characteristics of the variation of the relationship curves and the corresponding causes are analyzed. Finally, through the derivation of the formula, the reason for the decay of the excitation inrush current, the variation law of the decay rate of the excitation inrush current, and the factors affecting the decay rate of the excitation inrush current are analyzed. However, on this basis, the comparative analysis of the impact of excitation current and short-circuit current on the transformer winding is less studied. Literature [8] used a 15 KVA concentric double-winding single-phase transformer as a model using finite element analysis to analyze the magnetomechanical effects of transformer windings under the same conditions of excitation inrush current and short-circuit current. In [9], a two-dimensional and three-dimensional model of a three-phase transformer was established to analyze the forces and deformation of the transformer winding for different peak ratios of excitation inrush and short-circuit currents. In [10], a 50 MVA transformer is modeled and the peak excitation inrush current is obtained by transient simulation. The radial and axial forces on the transformer winding under the peak

and the deformation of the winding under electromagnetic forces are analyzed. The literature [11] begins to propose a model that takes into account the change in leakage inductance under transient conditions and takes the transformer geometry into account. The electromagnetic forces generated by short-circuit currents and excitation inrush are analyzed by combining the Jiles-Atherton model with a fixed-point iterative approach, taking into account the hysteresis characteristics of the core.

At present, most of the research on excitation inrush is the principle of analysis, identification, and inhibition, for short-circuit current and excitation inrush on the transformer winding impact involved and most of them only analyze the difference between the two generating electromagnetic force, for both the principle of comparison and generation of magnetic field difference is not described. In this paper, we will compare the principles of both, magnetic field distribution, electromagnetic force size, and other aspects of the short-circuit current and excitation inrush current of a comprehensive analysis. The field-path coupling method is combined with finite element analysis to model a 66.7 KVA transformer with dual windings and to analyze the electromechanical characteristics of the transformer windings during excitation inrush and short-circuit currents. A comprehensive comparison of the electromechanical characteristics of the windings produced by both is analyzed by the leakage magnetic fields generated by both and the effects of both on the windings and conclusions are drawn.

## II. FUNDAMENTAL ANALYSIS

### A. CALCULATION OF SHORT-CIRCUIT CURRENT

Short-circuit faults can be divided into three-phase, two-phase, and single-phase short-circuits, with three-phase short-circuits producing the largest fault currents. The short-circuit current can be obtained from the following formula.

$$\begin{cases} U = U_m \sin(\omega t + \theta) \\ = L_{sc} \frac{di_{sc}}{dt} + i_{sc} r_{sc} \\ i_{sc} = \frac{U_m}{\sqrt{r_{sc}^2 + (\omega L_d)^2}} \\ \left[ \sin(\omega t + \theta - \alpha) - \sin(\theta - \alpha) e^{-\frac{r_{sc}}{L_{sc}} t} \right] \end{cases} \quad (1)$$

where:  $i_{sc}$  is the symmetrical short-circuit current, A;  $L_{sc}$  is the system short-circuit inductance;  $r_{sc}$  is the short-circuit impedance value;  $U$  is the rated voltage, V.

Assuming  $r_{sc}/L_{sc} = 0$ , the short-circuit current is maximum when  $O$  is assumed to be 0.

$$\begin{cases} \sqrt{2} I_{sc} = \frac{100\sqrt{2}}{V_{sc}} I_n \\ I_{sc} = \frac{U_m}{\sqrt{r_{sc}^2 + (\omega L_d)^2}} \end{cases} \quad (2)$$

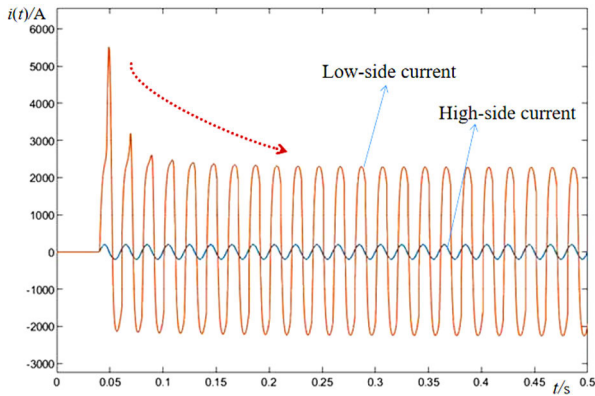


FIGURE 1. Short circuit high and low voltage winding current waveform.

As shown in Figure 1 is a single-phase transformer sudden short-circuit, high-voltage, and low-voltage side of the short circuit current waveform.

**B. CALCULATION OF EXCITATION INRUSH CURRENT**

Under normal stable operation, the no-load excitation current of a transformer is 2%-10% of the rated current, and for large transformers, it is even less than 1%. However, when the transformer is closed at no load or when the transformer is reclosed at fault, the excitation current will increase sharply due to the over-saturation of the iron core, forming an excitation inrush. Compared to the short-circuit current, the excitation inrush current has more high-frequency generation, the greater the hazard and other characteristics.

The transformer needs to go through a transient mode after reclosing before it can reach steady state mode. The voltage waveform, the phase angle at the moment of closing the switch, and the amplitude and direction of the remanence are the main factors in how long the transient mode can be maintained. When the secondary side is open, the current on the primary side may increase to more than ten times the rated transformer current. Neglecting the winding resistance values, the relationship between the voltage  $U_m \sin(\omega t + t)$  and the magnetic flux  $\phi$  can be expressed as

$$u = N \frac{d\phi}{dt} = U_m \sin(\omega_1 t + \alpha) \tag{3}$$

$N$  is the number of turns on the primary side of the winding, and the integration of the two side yields  $\phi$  as.

$$\phi = -\phi_m \cos(\omega_1 t + \alpha) + \phi_m + \phi_r \tag{4}$$

where  $\phi_r$  is the residual magnetism in the core, i.e.  $\phi(0) = \phi_r$ .

At the same time, the excitation inrush current is related to the primary side inductance  $L_T$  and the applied voltage  $u$  as follows.

$$u = -L_T \frac{di}{dt} \tag{5}$$

Therefore, the excitation inrush can be expressed as.

$$i = \frac{1}{L_T} \int U_m \sin(\omega t + \alpha) \tag{6}$$

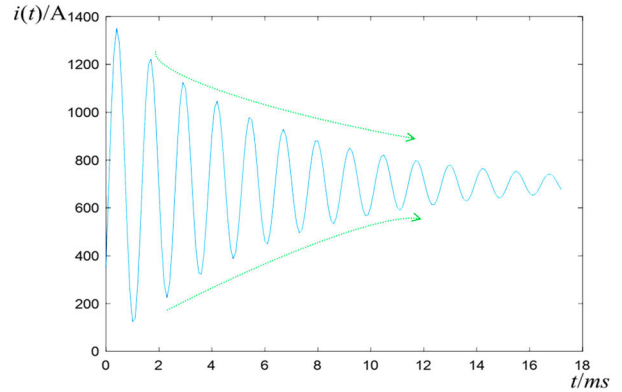


FIGURE 2. Typical inrush current waveform.

The maximum excitation inrush current can be expressed as.

$$I_{o \max} = \frac{N}{L_T} (2\phi_m + \phi_r - \phi_s) \tag{7}$$

where  $\phi_m = \frac{U_m}{\omega}$  represents the magnitude of the steady-state flux;  $\phi_s$  represents the saturation flux;  $\alpha$  denotes the closing phase angle;  $L_T$  is a no-load inductor.

Figure 2 shows the waveform of a typical excitation inrush of a transformer.

**C. LEAKAGE FIELD ANALYSIS AND CALCULATION**

When a large power transformer fails, the leakage field in the air gap will increase dramatically, and the rapidly increasing leakage field will lead to increased losses, component overheating, and even winding structure deformation, which seriously threatens the stability and reliability of the transformer as well as the operation of the entire power grid.

The path of the leakage flux is divided into four main components.

(a) Forming a closed circuit of the air gap between the winding.

(b) Flowing through the insulated parts of the upper end of the winding into the core clamp to form a closed circuit.

(c) Forming a closed circuit of the air gap between the high and low voltage windings.

(d) Forming a closed circuit of the transformer's tank.

The magnetic line of leakage will be bent at both ends of the winding, resulting in leakage of magnetic flux at both ends of the winding with axial and radial components. When a short-circuit or fault reclosing, short-circuit current or excitation inrush and spoke leakage component of the common role of production into axial and radial electromagnetic force, the huge electromagnetic force will destroy the structure of the winding as well as insulation, serious cases may make the transformer collapse.

Analysis of electromagnetic phenomena by solving Maxwell's system of equations under a given set of boundary

conditions.

$$\begin{cases} \nabla \times H = J + \frac{\partial D}{\partial t} \\ \nabla \times E = -\frac{\partial B}{\partial t} \\ \nabla \cdot D = \rho \\ \nabla \cdot B = 0 \end{cases} \quad (8)$$

The intrinsic structure relationship between them can be expressed as.

$$\begin{cases} B = \mu H \\ J = \sigma E \\ D = \epsilon E \end{cases} \quad (9)$$

where  $B$  is the magnetic induction strength vector;  $H$  is the magnetic field strength vector;  $J$  is the current density vector;  $E$  is the electric field strength vector;  $D$  is the potential shift vector;  $\rho$  is the charge density;  $\epsilon$  is the dielectric constant,  $F/m$ ;  $\mu$  is the permeability,  $H/m$ ;  $\sigma$  is the electrical conductivity,  $S/m$ .

#### D. ANALYSIS AND CALCULATION OF WINDING ELECTROMAGNETIC FORCE

The interaction between the current and the leakage field generates electromagnetic forces, and the magnitude of the electromagnetic forces is proportional to the square of the current so that the generation of short-circuit current or excitation inrush current will generate a huge electromagnetic force on the transformer winding. When the electromagnetic force is greater than the winding can withstand the limit, transformer damage will occur.

The electromagnetic force generated by the transformer windings is shown in equation (10).

$$\vec{F} = \vec{J} \times \vec{B} \quad (10)$$

where:  $J$  is the current density,  $A/m^2$ ;  $B$  is the leakage magnetic density,  $T$ .

The magnitude of the electromagnetic force is related to the axial and radial components of the leakage magnetic field, respectively. The radial and axial electromagnetic forces are generated under the action of the axial and radial leakage magnetic fields, respectively, as shown in equation (11).

$$\begin{cases} F_r = B_z \times J_\phi \\ F_z = B_r \times J_\phi \end{cases} \quad (11)$$

where:  $F_z$  is the axial electromagnetic force,  $N$ ;  $F_r$  is the radial electromagnetic force,  $N$ ;  $B_z$  is the axial leakage density,  $T$ ;  $B_r$  is the radial leakage density,  $T$ .

The diagram below shows the irradiation force due to excitation inrush and short circuit currents.

The short-circuit current affects both the inner and outer windings, while the inner winding is also subject to the support forces of the core, while the excitation inrush generated by energizing the transformer usually only affects the outer winding.

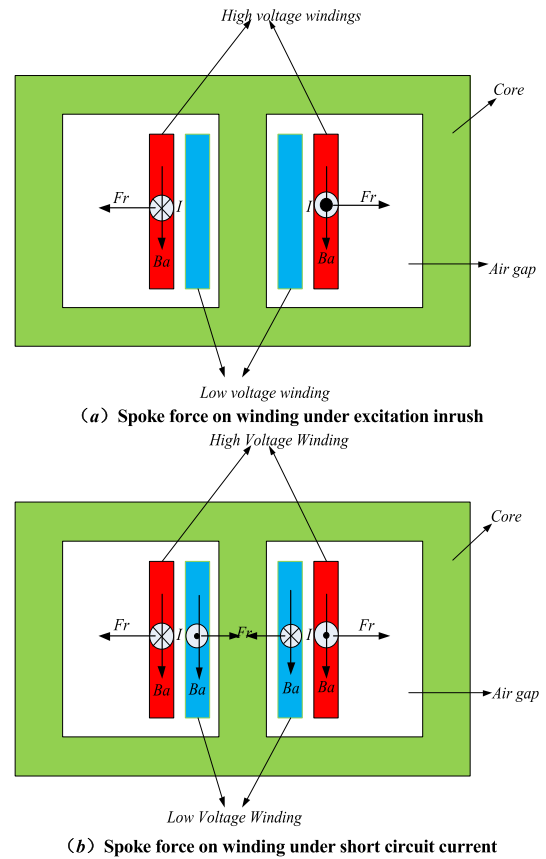


FIGURE 3. The radial force of winding under excitation inrush and short-circuit current.

The axially averaged magnetic density  $B_r$  can be expressed as.

$$\begin{aligned} B_z &= \mu_o H = \mu_o \frac{I_{d \max} \cdot W}{2H} \\ &= 0.4\pi \frac{I_{d \max} \cdot W \rho}{2H_K} \times 10^{-6} \end{aligned} \quad (12)$$

where:  $\rho$  is the Lowe's coefficient;  $H$  is the actual height of the winding,  $m$ ;  $H_K$  is the height of the winding reactance,  $m$ ;  $I_{d \max}$  is the maximum short-circuit current amplitude,  $A$ ;  $W$  is the number of rated turns.

So, the radial force can be expressed as:

$$F_r = 0.4\pi \frac{I_{d \max}^2 \cdot W^2 \rho D_{pi}}{2H_K} \times 10^{-6} \quad (13)$$

For concentric windings, the radial shear force is:

$$\sigma_x = \frac{F_x}{W \cdot S} = \frac{F_x}{2\pi W A_x} \quad (14)$$

where:  $A_x$  is the cross-sectional area of each turn of wire.

The direction of the axial force generated by the short-circuit current and the excitation inrush is the same, i.e. both compress the windings. The difference is that in the case of a short circuit, both the inner and outer windings are subjected to compression forces, while the electromagnetic forces generated by the excitation inrush only affect the outer

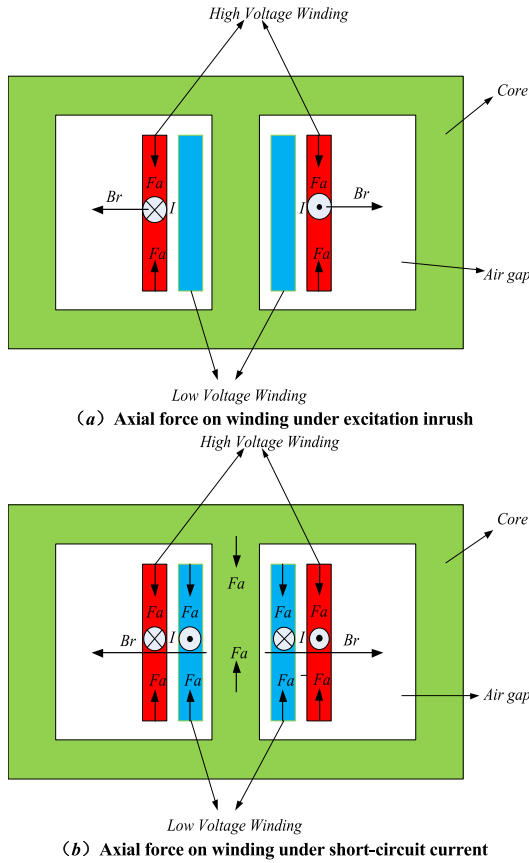


FIGURE 4. Axial winding forces under short-circuit current and excitation inrush.

windings. Figure 4 shows a diagram of the axial force on the winding.

The axial force at the ends of the transformer winding is directed towards the middle of the winding. Under the same conditions, the magnetic flux generated at the moment of reclosing the transformer is higher than that generated by the short-circuit current, therefore, the axial force generated by the excitation inrush is also higher than that generated by the short-circuit current.

The radial leakage density  $B_r$  can be expressed as.

$$B_r = 0.4\pi \frac{I_d \max \cdot W \rho_s}{2\lambda \times 10^8} \sum_1^{m-n} (a_m + a_{m-1}) W_m \quad (15)$$

where  $\lambda$  is the radial leakage width;  $\rho_s$  is the rock well coefficient of radial leakage;  $a_m$  is the maximum unbalanced ampere-turn percentage.

The axial electromagnetic force can be expressed as.

$$F_z = \frac{8.04}{\lambda \times 10^{11}} \times K_{ch}^2 K_I^2 (I_N W)^2 R_{pj} \rho_s \sum_1^{m-n} [(a_m + a_{m-1}) C_{pm}] \quad (16)$$

where  $C_{pm}$  is the percentage of regional turns.

TABLE 1. Main parameters of the transformer.

Parameters	Numerical
Rated capacity $S$ /(KVA)	66.7
Impedance percentage	10.56
Frequency $f$ /(Hz)	50
High and low voltage side rated voltage $U$ /(V)	219.4/219.4
High and low voltage rated current $I$ (A)	151.92/151.92
High and low voltage side turns	132/132

TABLE 2. Transformer model structural parameters.

Structural parameters	Numerical (mm)
Center distance of iron core column $L_1$	60
High and low voltage winding height $H_1$	100
High voltage winding inner diameter $L_2$	24
High voltage winding outer diameter $L_3$	24
Low voltage winding inner diameter $L_4$	18
Low voltage winding outer diameter $L_5$	22

The axial shear force is:

$$\sigma_y = \frac{1.256(K_{ch} K_I I_N)^2 W \rho_s \alpha_m l^2}{mn \times ab^2 \times \lambda \times 10^{10}} \quad (17)$$

where:  $a, b$  is the wire thickness and width.

### III. MODELING AND SIMULATION ANALYSIS

#### A. TRANSFORMER MODEL BUILDING AND RELATED PARAMETERS SETTING

A 66.7KVA single-phase double-winding transformer is used to analyze its magnetic leakage, electromagnetic force, and winding deformation. The main parameters of the transformer are shown in Table 1.

The transformer model's main structural parameters are shown in Table 2.

#### B. TRANSIENT SIMULATION OF WINDING ELECTROMAGNETIC CHARACTERISTICS UNDER THE INFLUENCE OF EXCITATION CURRENTS

##### 1) TRANSIENT SIMULATION OF WINDING ELECTROMAGNETIC FORCE UNDER THE EXCITATION INRUSH

When the transformer is closed at no load, the excitation inrush current reaches a maximum. The maximum excitation inrush current is reached when the transformer is closed with no load. With a residual flux of  $0.8 \phi_m$  and a closing phase angle of  $0^\circ$  or  $180^\circ$ . Figure 5 shows the variation curve of the transformer air gap leakage field.

Through the transformer winding air gap leakage magnetic field distribution curve can be seen, the air gap between each point of the leakage magnetic change trends are generally consistent, low-voltage winding and core between the air gap leakage magnetic density are smaller than the high and low-voltage winding air gap between the leakage magnetic degree. Between the low-voltage winding and the iron core,

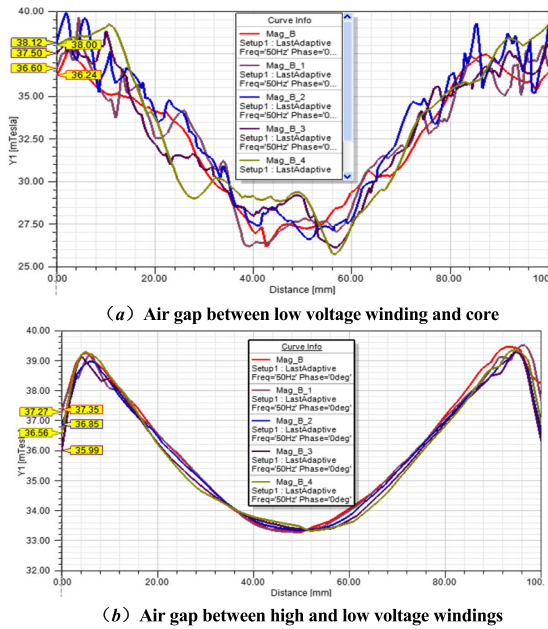


FIGURE 5. Air gap leakage field distribution.

the leakage magnetic density of both ends of the winding is the largest, with a maximum of  $39.6mT$ , and the minimum magnetic density in the middle is close to zero. Between the high voltage winding and the low voltage winding, the magnetic density at both ends of the winding is a maximum of  $40mT$ . As the electromagnetic force is interacted by the excitation current and the leakage magnetic field, the distribution of the electromagnetic force and the leakage magnetic field remains essentially consistent.

Figure 6 shows the volumetric force density cloud of the winding forces caused by the excitation inrush.

As can be seen from the diagram, the electromagnetic forces at the ends of the winding are greater than those in the middle, with a maximum value of  $203\ 960\ N/m^3$ .

Figure 7 shows the stress and displacement clouds of the windings.

From the figure can be obtained, in the action of the excitation current, the central winding by electromagnetic force is greater than the two ends, the maximum value reached  $10621Pa$ , winding the upper end of the most serious winding deformation, the maximum winding deformation for  $6.3511 \times 10^{-6}mm$ .

## 2) TRANSIENT SIMULATION OF WINDING ELECTROMAGNETIC FORCE UNDER SHORT-CIRCUIT CURRENT CONDITION

At the short-circuit occurrence of about  $0.01s$  [7], the short-circuit current will reach the peak of the first wave, the maximum short-circuit current is  $2050A$ , selected and the previous section of the same location to measure the leakage of magnetic density curve as shown in Figure 8.

Compared to the leakage field generated by the excitation inrush current, the leakage field generated by the short-circuit current is larger, and the variation is somewhat larger, and

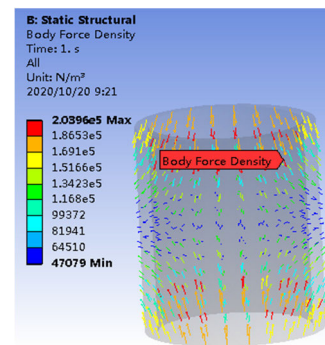


FIGURE 6. Volumetric force density vector diagram.

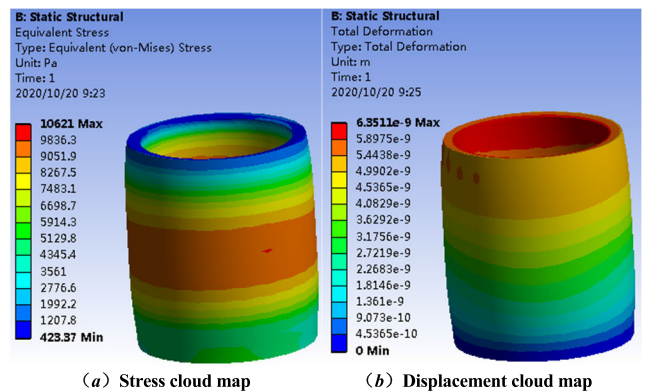


FIGURE 7. Winding stress and displacement cloud map.

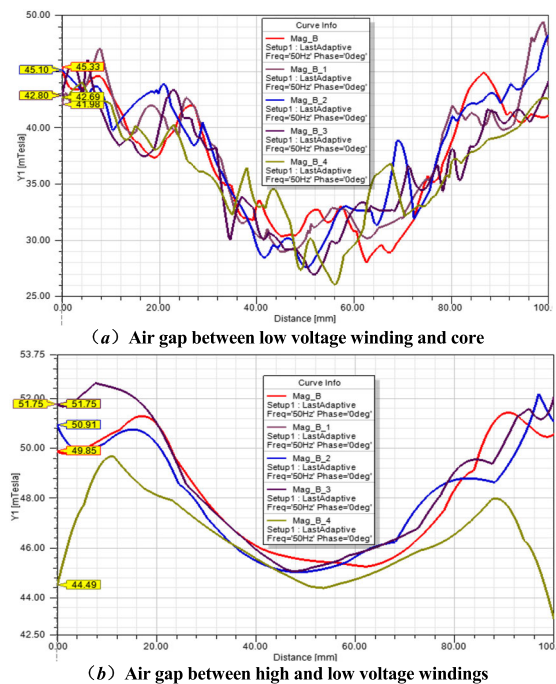


FIGURE 8. Air gap leakage field distribution.

the difference between different locations is also greater. The maximum magnetic leakage between the air gap between the low-voltage winding and the iron core reaches  $49.9mT$ ,

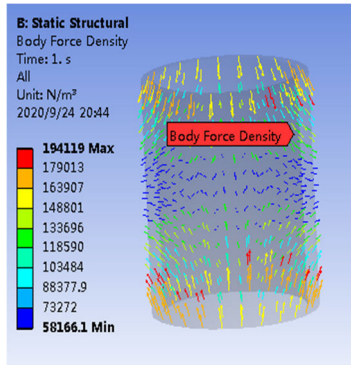


FIGURE 9. Volumetric force density vector diagram.

and the leakage between the high-voltage winding and the low-voltage winding air gap reaches  $53mT$ .

Figure 9 shows the volumetric force density of the transformer’s high-voltage winding for the influence of short-circuit currents.

The electromagnetic force in the middle of the winding is relatively small compared to the two ends of the winding due to the smaller leakage in the middle of the high voltage winding under short-circuit current condition. Compared to the electromagnetic force density under excitation inrush, the maximum electromagnetic force density generated by the short-circuit current is slightly larger, with a maximum value of  $194119N/m^3$ .

Figure 10 shows the stress cloud and displacement cloud of the high voltage winding under short circuit current condition.

As can be seen from the diagram, under the impact of the short-circuit current, the maximum force on the high-voltage winding, the maximum deformation variables are at both ends, the maximum force value of  $10324Pa$ .

### 3) TRANSIENT SIMULATION ANALYSIS OF WINDING ELECTROMAGNETIC FORCE UNDER THE INFLUENCE OF EXCITATION CURRENT

This paper mainly simulates and analyses the magnitude and direction of the electromagnetic force generated in the transformer winding by no-load and short-circuit excitation. The above simulation results lead to the values of the parameters affecting the winding in the case of short-circuit and no-load reclosing in Table 3 and the results of the comparison of the two.

From the above table, the peak excitation inrush current is only 73.55% of the peak short-circuit current, the electromagnetic force generated by the two on the high-voltage winding is almost equal, and the ratio of the two is 1.0507; the variation law of the leakage magnetism and the variation law of the excitation current are relatively close.

Through simulation analysis, it can be demonstrated that

(a) In the case where the peak excitation inrush current is only 70% of the peak short-circuit current, the magnitude of the electromagnetic force generated by the excitation inrush

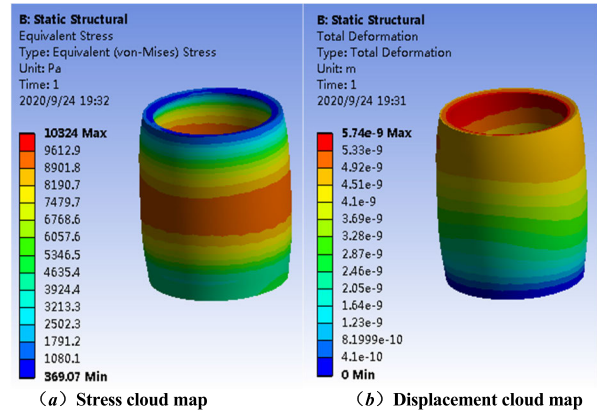


FIGURE 10. Winding stress and displacement cloud map of the high voltage winding under the influence of short circuit current.

TABLE 3. Effect of short circuit and reclosing on winding parameters.

Parameters	Short-circuit failure	No-load reclosing	Proportions
Maximum current $I_{max}/(A)$	2050.94	1475.37	0.7194
Maximum magnetic leakage of the air gap between windings $B_{1max}/(mT)$	53	40	0.7548
Maximum magnetic leakage of the air gap between winding and core $B_{2max}/(mT)$	49.9	39.6	0.7936
The maximum force $F_{max}/(Nm^{-3})$	194119	203960	1.0507
The average force $F_{ave}/(Nm^{-3})$	163142.6	162258.15	0.9946

current is approximately equal to the magnitude of the electromagnetic force generated by the short-circuit current.

(b) The two are again very different when analyzed from the point of view of the magnetization of the core as well as the magnetic field. When a short circuit occurs in a transformer, high currents are generated in both the high voltage and low voltage windings, whereas the excitation inrush current generated during no-load closing is only present on the high voltage winding side, a no-load condition.

(c) When the excitation amplitude is the same, the overall impact of the excitation inrush on the winding is slightly less than the impact of the short-circuit current, but in local locations, the magnetic field and electromagnetic force of the excitation inrush are greater than the impact of the short-circuit current.

### C. ANALYSIS OF WINDING DEFORMATION VARIABLES UNDER INRUSH CURRENT

The effects of excitation inrush current and short-circuit current on the transformer winding are not identical. To show the effect of both conditions on the windings clearly, a comparative analysis of the winding deformation variables through the X, Y, Z axis is presented below.

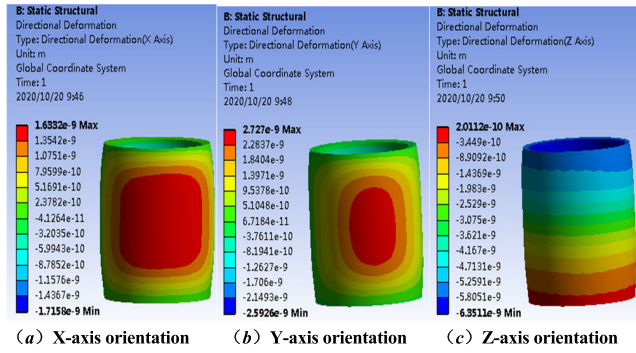


FIGURE 11. Deformation of the winding along with the three directions under excitation inrush current.

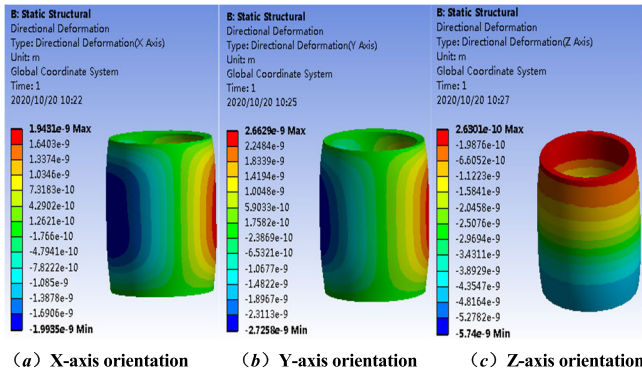


FIGURE 12. Deformation of the winding in three directions under short-circuit current.

Figure 11 shows the deformation of the winding in the X and Y-axis directions under the effect of the excitation inrush in the middle of the winding, and the deformation in the Z-axis direction is greater than the deformation in the other two directions.

Figure 12 shows the deformation of the high voltage winding along with the three directions under the influence of the short circuit current. Similar to the excitation inrush, the deformation of the winding under short-circuit current is mainly in the Z-axis direction, but the deformation caused by the short-circuit current to the winding is more uniform compared to the excitation inrush.

Excitation inrush current and short-circuit current on the transformer winding produced by the impact is not identical, to more clearly show the impact of both on the winding, the following will be through the X, Y, Z-axis three directional comparative analysis of the winding deformation. Table 4 shows the short-circuit current and excitation inrush current under the effect of winding deformation of comparative analysis.

As can be seen from the above table, the Z-axis direction of the excitation inrush current on the winding has a greater impact on the winding, the maximum winding deformation is about 1.11 times the short-circuit current condition, the average deformation is about 1.23 times the short-circuit current. In the role of the excitation inrush current, X-axis and Y-axis winding deformation variables

TABLE 4. Effect of short circuit and inrush current on winding parameters.

Unit ( $\times 10^{-4} mm$ )	X-axis	Y-axis	Z-axis
	orientation	orientation	orientation
Maximum deformation variable of winding under excitation inrush current $\Delta L_{imax}$	1.72	2.73	6.35
Maximum deformation variable of winding under short-circuit current $\Delta L_{smax}$	1.99	2.73	5.74
Specific value $\lambda$	0.86	1	1.11
Average deformation variable of winding under excitation inrush current $\Delta L_{aimax}$	0.65	1.13	4.28
Average deformation of winding under short-circuit current $\Delta L_{asmax}$	1.03	1.58	3.48
Specific value $\lambda$	0.63	0.72	1.23

TABLE 5. Model parameters of experimental transformer.

Parameters	Numerical values
Rated capacity $S_R$	66.7KVA
Rated voltage $U_R$	230.4V
Rated current $I_R$	151.92A
Rated magnetic density $B_R$	1.559T
Short circuit impedance $\rho_s$	10.56%
System resistance $R$	0.00748 $\Omega$
System inductors $L$	0.0888mH

are lower than the short-circuit current winding deformation variables. X-axis direction maximum deformation variable is about 0.86 times the short-circuit current condition, the average deformation variable is about 0.63 times the short-circuit current. Y-axis direction maximum deformation variable and the short-circuit current deformation variable is equal, the average deformation variable is about 0.72 times the short-circuit current condition.

The winding deformation curves in Figure 13 enable a comparative analysis of the difference between the electromagnetic forces generated by short-circuit current and excitation inrush on the transformer winding. In the Z-axis direction, the influence of the inrush current on the winding deformation is somewhat greater, the maximum winding deformation being approximately 1.11 times that of the short-circuit current. However, in both the X- and Y-axis directions, the winding deformation is slightly lower than the winding deformation under short-circuit current condition.

#### IV. EXPERIMENTAL VERIFICATION

By comparing the results of the simulation analysis in the previous section, the impact of the excitation inrush on the transformer winding can be determined. To further verify the accuracy of the simulation analysis results, experiments on the effect of excitation inrush current on the winding are conducted. The experimental transformer model is a



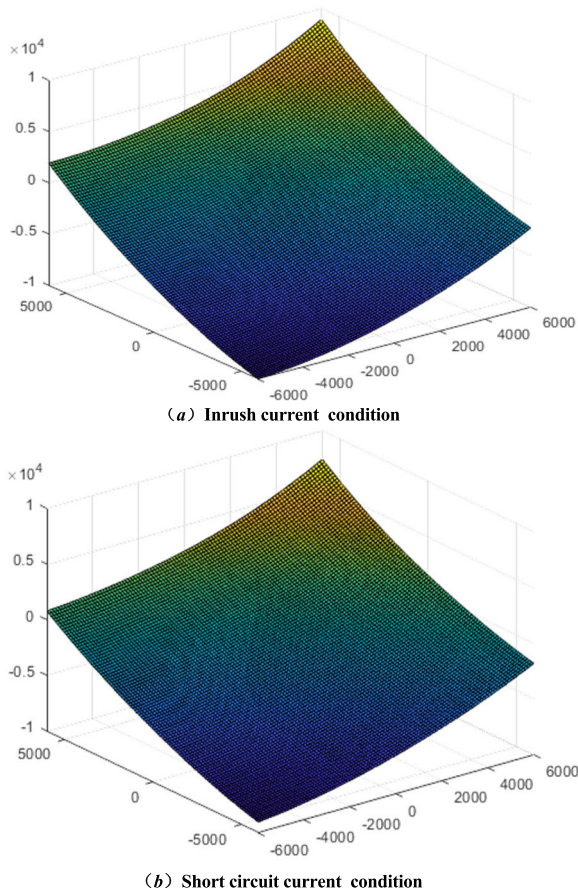


FIGURE 13. Winding deformation under excitation inrush and short-circuit currents.

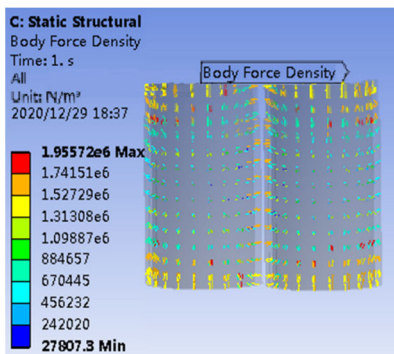


FIGURE 14. The transformer high-voltage winding volume force density cloud under excitation inrush.

single-phase dry-type transformer DG10-33.35/0.22 with the specific parameters shown in Table 5.

The simulation model is rebuilt according to the transformer to be tested in the laboratory. Figure 14 shows the transformer high-voltage winding volume force density under excitation inrush.

Since the leakage in the middle of the high voltage winding is smaller under the effect of excitation inrush, the electromagnetic force in the middle of the winding is smaller compared to the two ends. Compared to the electromagnetic force

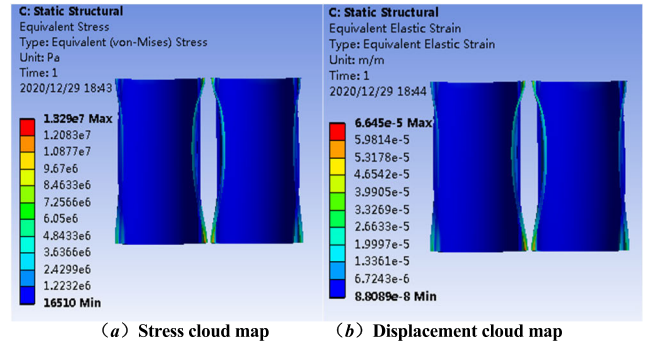


FIGURE 15. High-voltage winding stress and displacement cloud distribution.

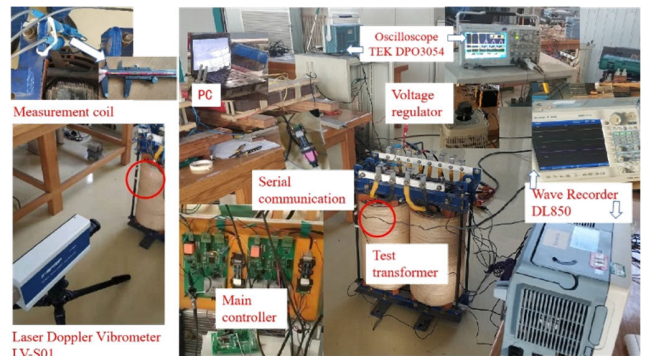


FIGURE 16. The experimental measurement site.

density under short-circuit current, the maximum electromagnetic force density generated by the excitation inrush is slightly larger, with a maximum value of up to  $1.96 \cdot 10^6 \text{ N/m}^3$ .

Figure 15 shows the stress cloud and displacement cloud distribution of the high-voltage winding.

As can be seen from Figure 15, the maximum value of the electromagnetic force on the high-voltage winding under the action of the excitation inrush can reach  $1.329 \cdot 10^4 \text{ KPa}$ , maximum shape variation up to  $6.645 \cdot 10^{-2} \text{ mm}$ .

To verify the simulation results, an experimental platform is built. During the experiment, the PC sends the phase angle setting value to the main control chip on the control board through serial communication. After the forward AC voltage crosses zero, the trigger angle of the forward thyristor is controlled to generate a different phase signal, and the reverse thyristor voltage crosses zero to trigger the renewal, while the AC contactor is turned on to keep the circuit connected. When the system is stabilized, the set value is sent to the master chip through the host computer to control the excitation loading values to form different remanences. Using Wave Recorder DL850 for current and voltage signal recording and storage, and oscilloscope TEK DPO3054 to display voltage and current signals, the multi-pass data acquisition function is used to collect circuit voltage signals throughout the experimental process. Furthermore, the test process uses the laser doppler micrometer LV-S01 to measure the winding deformation displacement under the influences of different remnant magnetism of the surge.

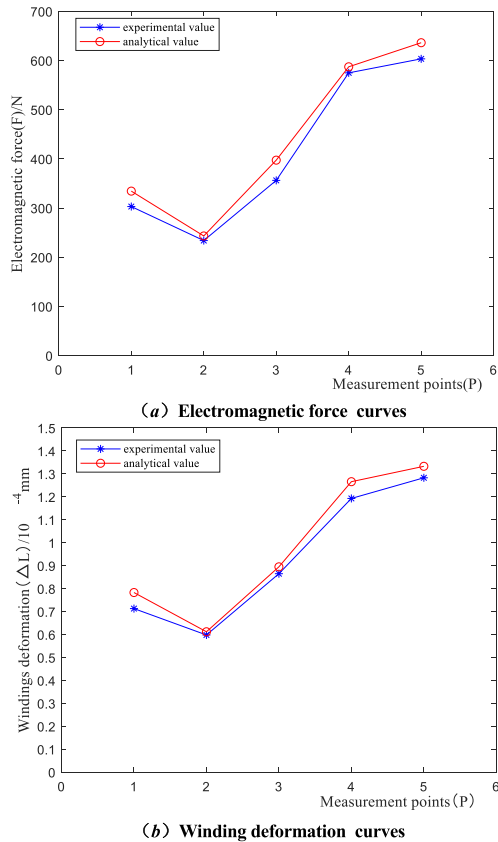


**FIGURE 17.** Comparison of experimental value and simulation value curves.

The experimental measurements site is shown in Figure 16.

The leakage density between the winding air gaps is measured using a measuring coil and the leakage waveform is displayed by a wave recorder DL850. A comprehensive analysis and calculation based on the experimentally detected leakage and current data are performed to derive the experimental calculated value of electromagnetic force.

Figure 17 shows the comparison curves of the results between the experimental and simulated values.

The comparison results in Fig. 17 show that the results of transformer winding deformation and electromagnetic force obtained from the simulation using the “field-road” coupling method are reliable, and prove the correctness of the conclusions of the simulation comparison analysis in this paper.

## V. CONCLUSION

The electromechanical stress characteristics generated by the excitation inrush current and the short-circuit current in the transformer windings are different. The electromagnetic forces generated by short-circuit currents have an impact on both the high and low voltage windings of the transformer, whereas the electromagnetic forces generated by the excitation inrush only act on one side of the high voltage winding. As the excitation inrush causes the transformer core to be oversaturated and the permeability to be reduced, the component generated by the leakage flux can be ignored. Therefore,

when analyzing the transformer windings under the excitation inrush, the field component generated by the current in the high voltage winding is generally only considered.

As the duration of the excitation inrush is significantly higher than the short-circuit current, even if the peak of the excitation inrush is 30% lower than the peak of the short-circuit current, the magnitude of the electromagnetic force generated by the two conditions is essentially the same, and compared with the operation of the short-circuit current, the excitation inrush will produce greater displacement in the winding, so the danger to the transformer of the excitation inrush cannot be ignored.

The magnetic lines of force are bent at the ends of the windings and have their greatest value. The leakage in the core window is greater than outside the window due to the influence of the yoke etc. The leakage caused by different faults is different and the path of the leakage flux is also different. The leakage from an excitation inrush is slightly greater than that from a short circuit, resulting in a somewhat greater electromagnetic force.

In addition, when a short circuit occurs, the protection device will act quickly and the fault can be cleared within a few tens of milliseconds, but the excitation inrush not only lasts for a long time and occurs with high frequency, but often the system does not consider it to be a fault. As the occurrence of excitation inrush is not considered a fault, the frequency of excitation inrush is much higher than the frequency of short-circuit currents. Many power transformers under no-load conditions frequently energized insulation damage accidents have also shown that the impact of excitation inrush current is not weaker than short-circuit current or even greater than the impact of short-circuit current.

Therefore, through this paper on the power transformer winding in the excitation inrush current and short-circuit current excitation under the simulation results of the comprehensive comparison, clear the two on the power transformer electromechanical performance of the impact; at the same time, in the short-circuit current and excitation inrush current in the same amplitude or excitation inrush current amplitude slightly lower, analysis of its impact on the same side of the winding, can better determine the cause of winding deformation, to take the corresponding preventive and control measures, effectively extend the operating efficiency and service life of power transformers. Effectively extend the operating efficiency and service life of power transformers.

## REFERENCES

- [1] S. Lan, Z.-P. Hu, F.-W. Liao, and Y.-B. Yuan, “Radial stability of transformer low voltage windings under sudden short-circuit,” *Dianji yu Kongzhi Xuebao/Electr. Mach. Control*, vol. 22, no. 5, pp. 19–24, 2018.
- [2] G. B. Kumbhar and S. V. Kulkarni, “Analysis of short-circuit performance of split-winding transformer using coupled field-circuit approach,” *IEEE Trans. Power Del.*, vol. 22, no. 2, pp. 936–943, Apr. 2007.
- [3] H.-M. Ahn, J.-Y. Lee, J.-K. Kim, Y.-H. Oh, S.-Y. Jung, and S.-C. Hahn, “Finite-element analysis of short-circuit electromagnetic force in power transformer,” *IEEE Trans. Ind. Appl.*, vol. 47, no. 3, pp. 1267–1272, May 2011.

- [4] S. Wang, S. Wang, N. Zhang, D. Yuan, and H. Qiu, "Calculation and analysis of mechanical characteristics of transformer windings under short-circuit condition," *IEEE Trans. Magn.*, vol. 55, no. 7, pp. 1–4, Jul. 2019.
- [5] A. Bakshi, "Effect of width of axial supporting spacers on the buckling strength of transformer inner winding," *IEEE Trans. Power Del.*, vol. 34, no. 6, pp. 2278–2280, Dec. 2019.
- [6] J. V. Leite, A. Benabou, and N. Sadowski, "Transformer inrush currents taking into account vector hysteresis," *IEEE Trans. Magn.*, vol. 46, no. 8, pp. 3237–3240, Aug. 2010.
- [7] J. Feng, P. Zhang, and Z. Chen, "Research on inrush current mechanisms of single phase transformers," *J. Phys., Conf. Ser.*, vol. 1026, May 2018, Art. no. 012030.
- [8] R. Guimarães, A. C. Delaiba, A. J. P. Rosentino, E. Saraiva, and J. C. de Oliveira, "Electromechanical stress in transformers caused by inrush and short circuit currents," *J. Brazilian Soc. Mech. Sci. Eng.*, vol. 37, no. 1, pp. 243–253, Jan. 2015.
- [9] M. Steurer and K. Frohlich, "The impact of inrush currents on the mechanical stress of high voltage power transformer coils," *IEEE Trans. Power Del.*, vol. 17, no. 1, pp. 155–160, 2002.
- [10] W. S. Fonseca, D. S. Lima, A. K. F. Lima, M. V. A. Nunes, U. H. Bezerra, and N. S. Soeiro, "Analysis of structural behavior of Transformer's winding under inrush current conditions," *IEEE Trans. Ind. Appl.*, vol. 54, no. 3, pp. 2285–2294, May 2018.
- [11] G. B. Kumbhar and S. M. Mahajan, "Analysis of short circuit and inrush transients in a current transformer using a field-circuit coupled FE formulation," *Int. J. Electr. Power Energy Syst.*, vol. 33, no. 8, pp. 1361–1367, Oct. 2011.
- [12] J. Mitra, X. Xu, and M. Benidris, "Reduction of three-phase transformer inrush currents using controlled switching," *IEEE Trans. Ind. Appl.*, vol. 56, no. 1, pp. 890–897, Jan. 2020.
- [13] L. Petrescu, E. Cazacu, V. Ioniță, and M.-C. Petrescu, "An experimental device for measuring the single-phase transformers inrush current," *Sci. Bull. Electr. Eng. Fac.*, vol. 19, no. 1, pp. 18–22, Apr. 2019.
- [14] A. M. Sobrinho, J. R. Camacho, J. A. Malagoli, and A. C. F. Mamede, "Analysis of the maximum inrush current in the optimal design of a single phase transformer," *IEEE Latin Amer. Trans.*, vol. 14, no. 12, pp. 4706–4713, Dec. 2016.
- [15] P. Huang, C. Mao, and D. Wang, "Analysis of electromagnetic force for medium frequency transformer with interleaved windings," *IET Gener., Transmiss. Distrib.*, vol. 11, no. 8, pp. 2023–2030, Jun. 2017.
- [16] Y. Wang, J. Zhang, B. Zhou, Y. Wang, Y. Ni, and J. Pan, "Magnetic shunt design and their effects on transformer winding electromagnetic forces," *Iranian J. Sci. Technol., Trans. Electr. Eng.*, vol. 43, no. 1, pp. 97–105, Mar. 2019.



**CHENCHEN ZHANG** was born in Henan, China, in 1995. He received the bachelor's degree in engineering from Tianjin Chengjian University, in 2019, where he is currently pursuing the master's degree in engineering. His research interests include dynamic measurement and control, intelligent diagnosis and repair, and remanufacturing technology.



**WENQI GE** was born in Hebei, China, in 1986. She received the B.S. degree in electrical engineering and automation and the Ph.D. degree in electrical engineering from the Hebei University of Technology, China, in 2009 and 2014, respectively. From 2014 to 2016, she held a postdoctoral position with the Mechanical Engineering Department, Hebei University of Technology. Since July 2016, she has been an Instructor with the School of Control and Mechanical Engineering, Tianjin Chengjian University. Her research interests include engineering electromagnetic field and electrical engineering power systems.



**YI XIE** was born in Anshun, Guizhou, China, in 1996. She received the B.S. degree in electrical engineering and automation from Tianjin Chengjian University, in 2018, where she is currently pursuing the master's degree in engineering. Her research interests include grid analysis and drone patrol inspections.



**YINGYING LI** received the degree in precision instrumentation and machinery from Tianjin University. She is currently pursuing the Ph.D. degree with the Tianjin Research Institute of Construction Machinery. She is also a Researcher-Level Senior Engineer and the Deputy Director of technology with the Tianjin Research Institute of Construction Machinery. She has presided over and participated in nearly ten national key projects and horizontal projects. She has presided over the science and technology support projects of the 12th Five-Year Plan. She published 26 high-level papers, holds five patents, and five standards. Her main research is the energy-saving technologies for machinery, product development, and basic common technology research directions for construction machinery. She received the First-Class Prize for scientific and technological progress at the provincial and ministerial level in China.

...